# CIVA as an Aid to Understanding Ultrasonic Anisotropy in Steel

Ed Ginzel [1]

[1] University of Waterloo, Waterloo, Ontario, Canada
e-mail: eginzel@mri.on.ca

2024.02.20

**Abstract**
Standard calibration blocks to assess beam paths and configure data displays using ultrasonic instruments use low carbon steel with isotropic acoustic properties. However, industry is trending towards the use of high tensile steels where the acoustic properties are anisotropic. When an ultrasonic system, calibrated on an isotropic steel reference block, is used on anisotropic steels, the beam can be bent, skewed and attenuated so that the reference setup is rendered useless. CIVA simulation software can be used to aid in understanding the effects on the data displays. As well, CIVA can help to demonstrate the degree of change that can occur when the acoustic velocities are established for the fast and slow shear modes in an anisotropic steel.

**Keywords:** CIVA, ultrasonic, anisotropy, TMCP, birefringence

## 1. Introduction

ISO 2400[1] is the ISO Specification for the ultrasonic testing calibration block No. 1. This reference block was more commonly known as the IIW block and is used universally to verify ultrasonic parameters such as refracted beam angle, instrument linearity, probe exit point and to set the instrument range for inspections in both longitudinal and shear modes. The material is specified as steel grade S355J0 with strict controls on heat treatment so that the determined longitudinal wave velocity shall be 5920 m/s $\pm$30 m/s and the transverse wave velocity shall be 3255 m/s $\pm$15 m/s. The same requirements are made for the Calibration block 2 (ISO 7963[2]) and the Phased-array calibration block (ISO 19675[3]). The heat treatment of these blocks ensures that the acoustic velocities are essentially isotropic (i.e. the same in all directions). However, when steels are made in the steel-mills, the rolling and heat treatment processes are not concerned with acoustic properties being uniform in all directions. As a result, there can be differences in the acoustic properties, in particular acoustic velocities dependant on the direction. In many cases, the differences are small and assumptions made when calibrating on the isotropic reference blocks are adequate to provide accurate positioning of indications in an ultrasonic inspection.

Some steels are made using rolling and heat treatment that intentionally makes the steel acoustically anisotropic; i.e., having different acoustic velocities in different directions. The process used to fabricate these steels is often referred to as TMCP (Thermo-Mechanical Controlled Process). These steels offer low temperature toughness and good weldability and as such, are found to be useful for off-shore structures and ship-building [4]. As well, TMCP steels are now commonly used for plate used to fabricate pipe used in pipeline construction.

In addition to the fact that the longitudinal wave velocity changes with direction, anisotropic steels can be characterised by the fact that two separate shear modes exist with polarisation of particle displacements at right angles to each other. This splitting of the shear components is a result of differences in stiffness in the lattice structure and the effect is called birefringence. In

some materials (e.g. quartz) the resulting velocity differences can be extreme. This was illustrated using the photoelastic effect [5]. Because shear waves can have two separate velocities in these materials, it is not possible to use Snell's law to calculate a single refracted angle, as would be done when inspecting isotropic steel. Either the fast or the slow shear mode could dominate the energy flow, depending on the grain structure of the material being tested.

Although acoustic birefringence can be caused by applied or residual stress, the birefringence we are concerned with is attributed to texture. Keiji [4] uses the ratio of the apparent shear velocities in the longitudinal and circumferential directions to rate the degree of anisotropy. This seems to be somewhat qualitative in that the values are derived from a single pitch-catch V path of the bulk shear waves or a single position through the thickness of a plate with a contact shear wave probe. As well, not all forms of steel can be classified as having a longitudinal and circumferential direction. Carvajal [6] indicates a more practical parameter to assess; the Acoustic Birefringence Coefficient. The Birefringence Coefficient B is quantified as the ratio of the difference of fast and slow shear velocities to their average.

The acoustic velocities (longitudinal and slow and fast shear) and the density of a material can be used to establish the stiffness tensors. Using stiffness tensors, the Christoffel equations can be used to derive the slowness curves that provide an indication of the acoustic velocities with respect to the crystal lattice planes.

In this paper we use the ability of CIVA simulation software to calculate velocities from Christoffel equations. Working from typical values of acoustic velocities measured in TMCP steels in line pipe, the stiffness tensors in the CIVA elastic constants matrix are adjusted to provide similar acoustic velocities in simulated materials. The effect of anisotropy on the simulated inspection results is then demonstrated.

## 2. Anisotropic Materials in CIVA

The CIVA help menu provides a good description of how materials' stiffness properties are to be used in the stiffness matrix. The user must first provide a material density and then select a crystal symmetry that approximates the material they are working with. Once the symmetry option has been selected, the user needs to enter the appropriate elastic constants in GPa (GigaPascals).

The number of required values of the stiffness matrix varies with the type of symmetry:

 • Isotropic (2 values): c11, c66

 • Cubic (3 values): c11, c12, c44

 • Transversely isotropic (5 values): c11, c12, c13, c33, c44

 • Orthotropic (9 values): c11, c12, c13, c22, c23, c33, c44, c55, c66

 • Monoclinic (13 values): c11, c12, c13, c16, c22, c23, c26, c33, c36, c44, c45, c55, c66

 • Triclinic (21 values): c11, c12, c13, c14, c15, c16, c22, c23, c24, c25, c26, c33, c34, c35, c36, c44, c45, c46, c55, c56, c66

CIVA provides the matrix with the appropriate cells open for values to be entered. When a particular symmetry is selected, the cells not available for entry have values calculated based on the cells with values entered. The generic layout of the matrix is seen Figure 1.

| C11 | C21 | C31 | C41 | C51 | C61 |
|-----|-----|-----|-----|-----|-----|
| C12 | C22 | C32 | C42 | C52 | C62 |
| C13 | C23 | C33 | C43 | C53 | C63 |
| C14 | C24 | C34 | C44 | C54 | C64 |
| C15 | C25 | C35 | C45 | C55 | C65 |
| C16 | C26 | C36 | C46 | C56 | C66 |

**Figure 1        Generic layout for Stiffness matrix**

For the purposes of this demonstration, it was considered that it would be appropriate to configure a matrix that closely approximates low-carbon isotropic steel. Elastic constants of materials are not frequently published. A good starting point was found in a paper by Spalthoff et al [7] where a full set of matrix values was provided by the authors using both ultrasonic and crystallographic texture[1] methods. Using the stiffness constants derived from the Hill method of averaging the texture, the 9 values for the orthotropic symmetry were entered in the CIVA stiffness matrix and the Slowness Curves were visualised as seen in Figure 2.
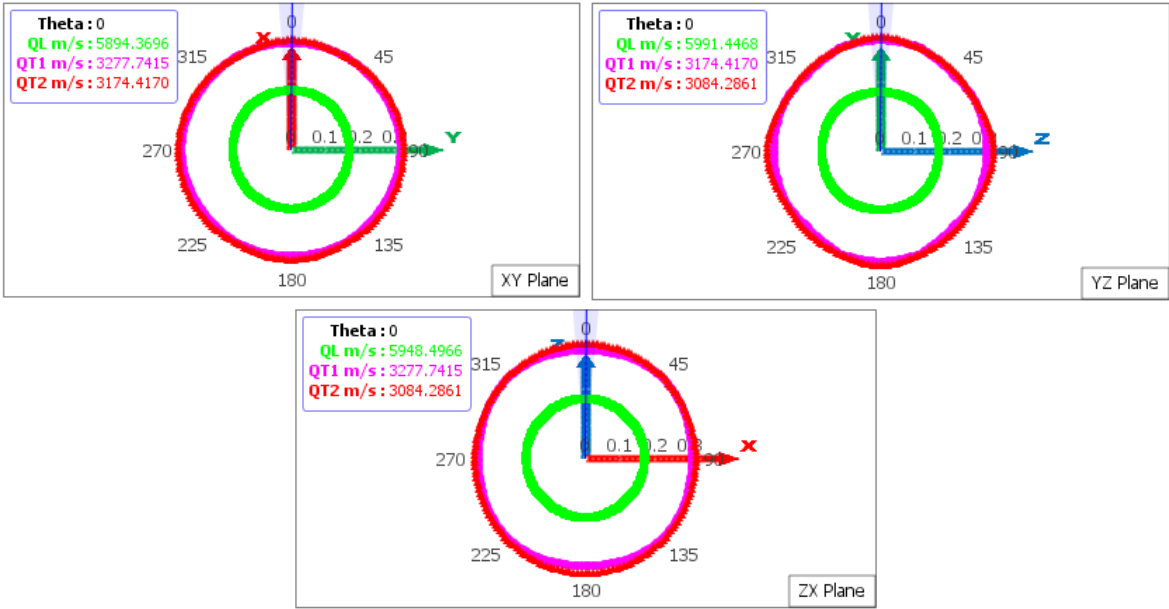


**Figure 2        Slowness curves for rolled low-caron steel**

---

[1] In a polycrystalline material such as a metal, axes of the grains are randomly oriented or their orientation can be non-random. If there is a non-random (preferred) orientation, then the material is considered to have crystallographic texture.

Slowness curves plot the inverse of velocity (i.e. μs/mm) in a plane of the material. Figure 2 illustrates a low level of anisotropy with respect to the longitudinal mode (green circles) and a slightly more pronounced anisotropy and birefringence of the shear modes (red and purple circles).

For the purpose of modelling a TMCP-type steel, the assumption was made that the material would approximate a steel with transversely isotropic symmetry. It was elected to assign the X-direction of the CIVA model as the rolling axis. For transversely isotropic materials only 5 stiffness values are required; c11, c12, c13, c33, c44. Using the values for these cells that were entered in the orthotropic sample, a similar small anisotropy resulted in the XZ and XY planes; however, in the YZ plane the velocities in the transversely isotropic model were uniform around the 360° slowness plot.

The method used to determine acoustic velocities to assess anisotropy is carried out essentially the same way by all users. Spalthoff used a rolled plate and cut and milled rectangular blocks with parallel sides. Ginzel & Ginzel [8] prepared parallel surfaces at angles in pipe (Figure 3). This became the standard configuration for assessments required in the DNV off-shore inspection of pipeline girth welds.
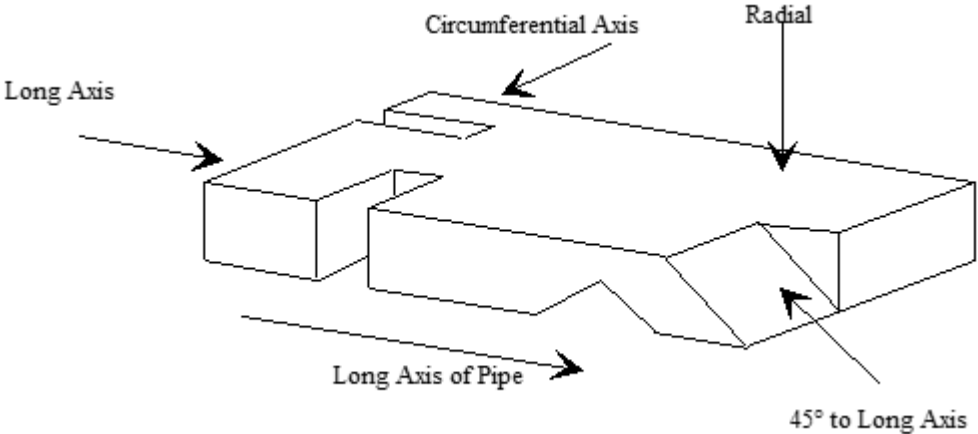


**Figure 3        Configuration of Slots Machined for Velocity Determination**

## 3. CIVA Velocity Assessment of Anisotropic Steels

In the 2023 version of CIVA simulation software, a new feature was added that has greatly assisted in modelling of anisotropic materials. Prior to 2023 the only way of assessing acoustic anisotropy in a metal was to have access to the Eddy Current Testing module in CIVA and make an EMAT-style probe to excite SH shear mode in the metal. The most recent version of the software now provides the option to use a contact piezoelectric-style shear wave probe with option to activate vibration in either the X or Y axis. By rotating the probe on the surface of a simulated anisotropic steel, it is possible to simulate generation of both the slow and fast modes.

Using the concepts identified in Figure 3, a method of confirming the slowness curves predicted by the stiffness matrix was configured. A model of a piece of steel was made with angled surfaces having parallel surfaces on which to make velocity measurements. Angles were arranged from 0° to 90° so that a contact shear wave probe could be placed on the surfaces to

obtain a fast and slow shear mode signal.  The angled steps seen in Figure 4 are arranged so that velocities in the X-Z plane can be determined.
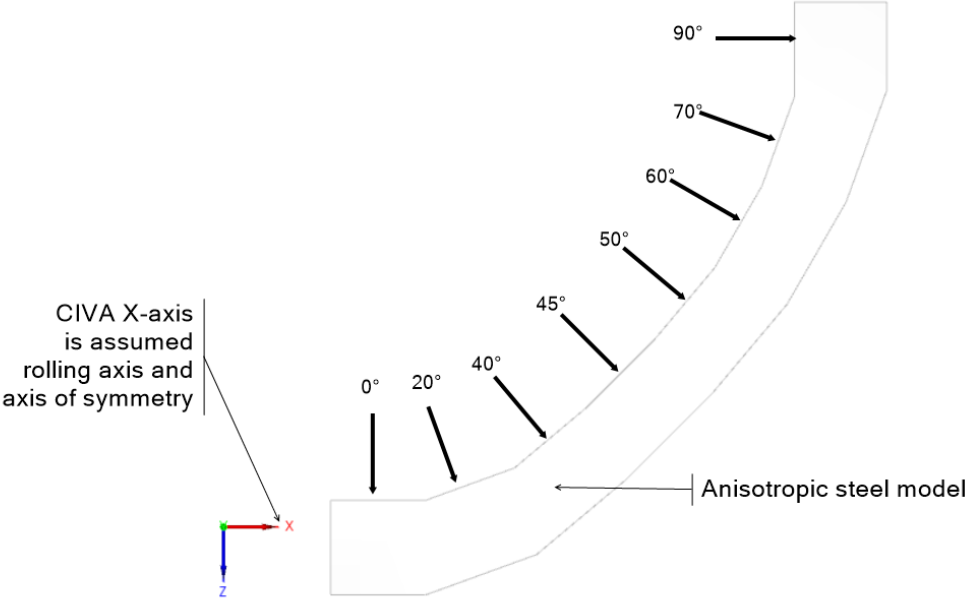


**Figure 4        Angled steps simulated in transversely symmetric anisotropic steel**

An A-scan was generated at each angular step with the probe oriented such that the vibration direction of the probe was at 45° to the XZ plane.  This ensured that both modes could be detected.  Figure 5 illustrates the setup for the first position with the first two backwall signals displayed.
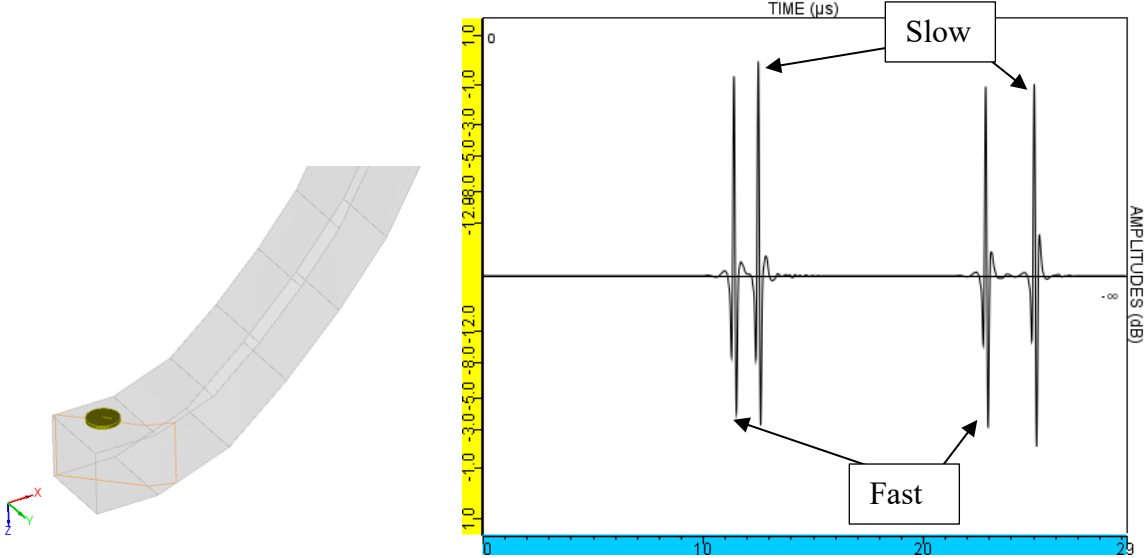


**Figure 5        Obtaining fast and slow shear mode velocities**

The time interval measured on the A-scans between each mode was then divided into the total travel distance (i.e. twice the wall thickness) to obtain the acoustic velocity. Results are tabulated in Table 1; there they are compared to the calculated values in the slowness curves.

**Table 1          Comparing Velocities – Christoffel versus A-scan**

| Sample | Angle | Thickness | Christoffel fast | Christoffel Slow | UT-Fast | UT Slow |
|---|---|---|---|---|---|---|
| 1 | 0 | 20 | 3489.91 | 3182.48 | 3493.45 | 3182.18 |
| 2 | 20 | 18.77 | 3368.06 | 3220.39 | 3366.82 | 3219.55 |
| 3 | 40 | 17.05 | 3311.59 | 3212.53 | 3320.35 | 3204.89 |
| 4 | 45 | 16.7 | 3341.95 | 3202.9 | 3346.69 | 3202.30 |
| 5 | 50 | 16.68 | 3368.92 | 3212.14 | 3373.10 | 3213.87 |
| 6 | 60 | 17.12 | 3418.12 | 3274.83 | 3424.00 | 3279.69 |
| 7 | 70 | 17.85 | 3457.45 | 3370.26 | 3442.62 | 3377.48 |
| 8 | 89.5 | 19.3 | 3491.46 | 3489.21 | 3477.48 | 3477.48 |

Values in Table 1 for the Fast and Slow shear velocities have the Christoffel estimates within less than 0.5% of the measured values.

## 4. CIVA Beam modelling of Anisotropic Steels

Phased-array probe delay laws were configured for 3 beams in isotropic steel (45°, 57.5°, 70°). Without adjusting the delays, the probe was then placed on an anisotropic steel with a birefringence coefficient of 13%.

Single rays indicate refracted angles for the isotropic steel in Figure 6, whilst double rays are calculated for the Snell's law values for the anisotropic steel.
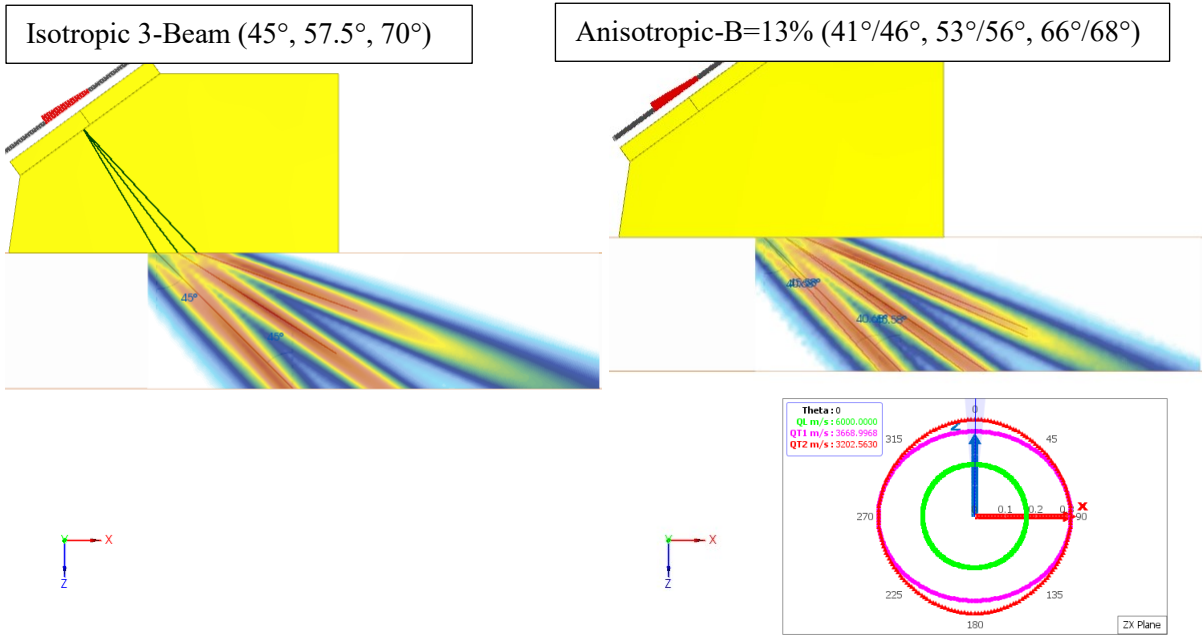


**Figure 6          Compare delay laws in isotropic and anisotropic steels**

If this was a rolled plate and the scanning was carried out at right angles to the X-axis, the angle beams would be directed perpendicular to the axis rolling axis (assumed to be parallel to the X-axis).  Shear velocities in this plane remain approximately constant for the fast and slow values at each angle; however, at 3668m/s, the value is significantly higher for the fast shear than the 3230m/s used for the delay laws made using the isotropic steel.  And although the value of the slow shear, at 3204m/s, is slightly lower than the isotropic condition, the energy flow sees the fast shear dominate the refraction.  Using the same 3 delay laws used in Figure 6, we see in Figure 7 that the resulting refraction is significantly increased, to the extent that the nominal 70° beam is totally internally reflected.  The "effective" angles are now well away from the nominal values that were made using isotropic steel velocities.
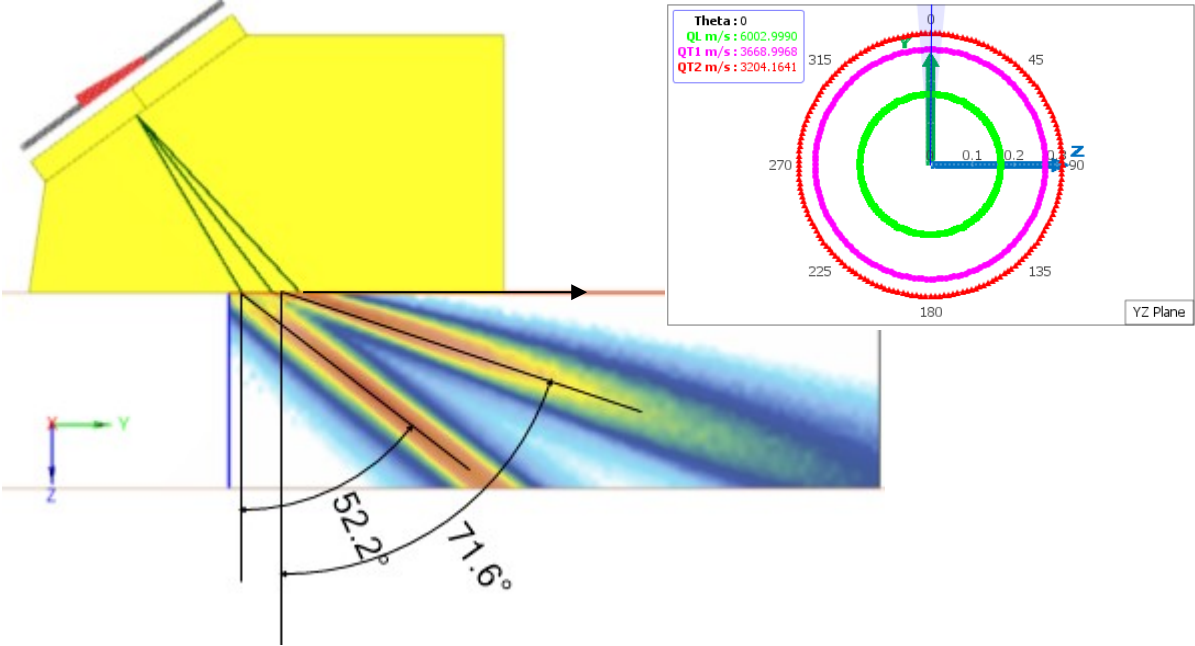


**Figure 7        Intended 3 beam refraction in high birefringence anisotropic steels**

When the acoustic velocity of the shear wavefront is increased by the anisotropy, as in Figure 7, the standard instrument display results in an incorrect positioning of features.  This was identified by Holloway [10] [11] as the "melting S-scan".  Standard phased-array instrument displays are based on inputs about nominal angle and velocities entered by the operator.  Using the display from Holloway [10] in Figure 8, the mispositioning on the standard S-scan display can be explained.  The S-scan sweep is intended to be 40° to 70°.  The response from the root weld cap is plotted along the nominal 63° path and at a distance well beyond the weld cap.  In fact, the signal has occurred earlier in time than the plotted location and at an angle higher than the delay laws have identified.  It must be kept in mind that the S-scan display maps the angles based on the delay laws rather than the actual refracted angles in the material.
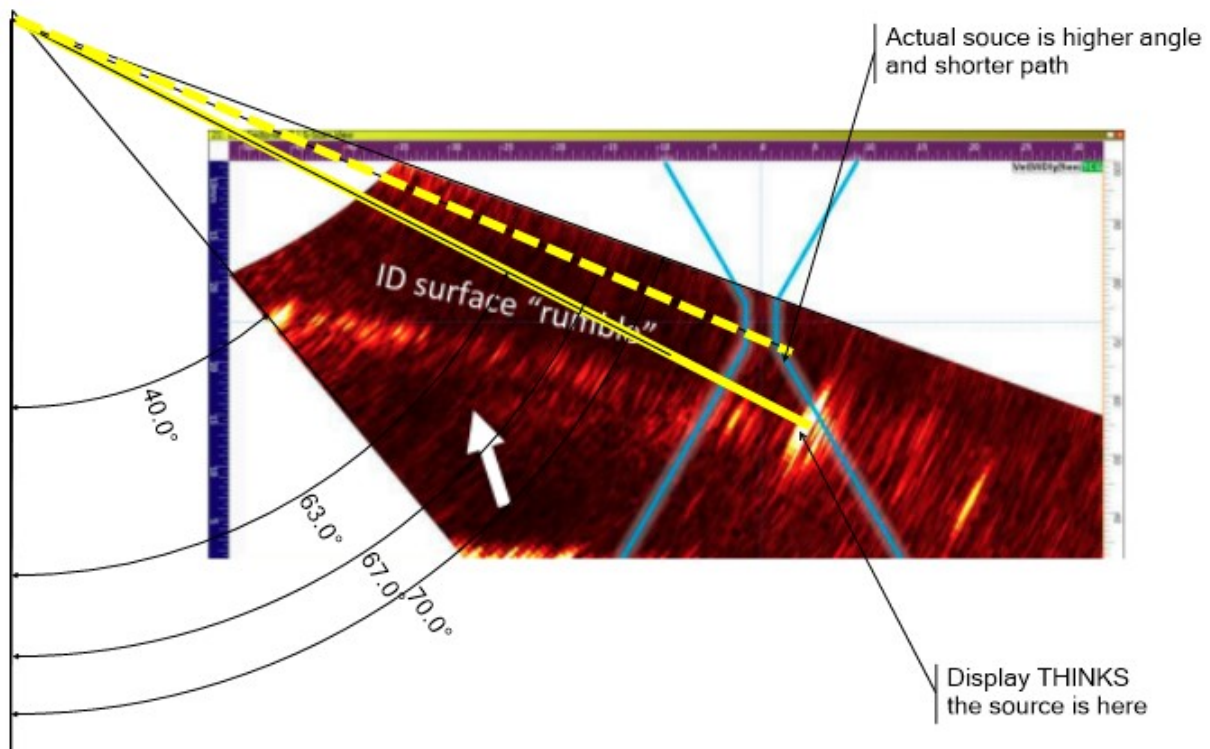
**Figure 8        Holloway's "Melting S-scan"**

## 5. CIVA Inspection Imaging in Anisotropic Steels

Of course, when ultrasonically testing a weld in steel, the degree of anisotropy is not known and as described, it can be a variable dependant on angle and plane. Estimating the actual refracted angle is described by Keiji [4] is also described in the old DNV Classification Notes 7 [12], where in 2012 they added guidance for testing TMCP steels. They describe the pitch-catch arrangement of 2 shear wave probes and use a simple formula to estimate the refracted angle α:

$$\tan^{-1} \alpha = \frac{S}{2t}$$

- where S is the probe spacing measured at the exit points of the wedges and t is the material thickness.

A pitch-catch arrangement was configured in CIVA on a 30mm isotropic steel plate and a pair of 60° probes. A parametric study was run by placing the probe-wedges facing each other and then moving them apart and collecting the waveforms. The resulting amplitude trend was plotted (see Figure 9) and the location of the maximum response assessed for the probe-centre spacing. Using the equation from Classification Notes No. 7, the refracted angle is estimated at 59.5°.
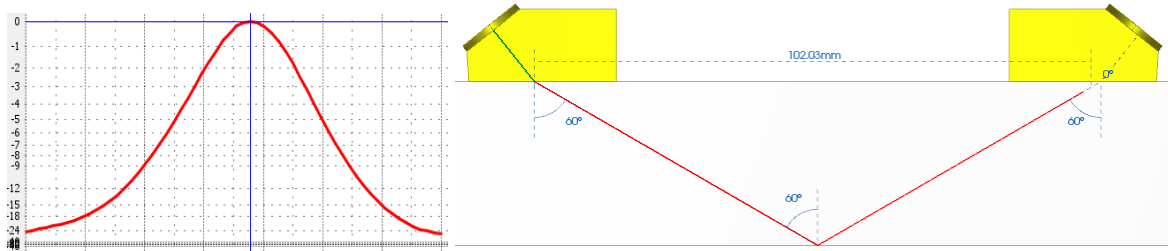
**Figure 9**      **Calculating the refracted angle in isotropic steel as per DNV CN 7**

When we use the same process for the probe on the 30mm thick anisotropic steel in the X-plane (assumed rolling plane) the equation indicates 58.4° as the refracted angle. This is closer to the fast shear ray-path at 58.6° indicated in Figure 10 and there is no indication of a double peak in the echo-dynamic response that would suggest the presence of a slow shear component.
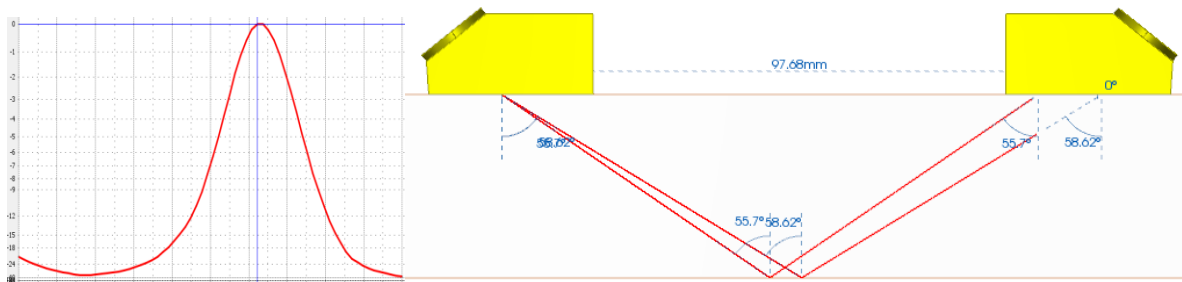


**Figure 10**      **Calculated 58.4° angle for nominal 60° in anisotropic steel along rolling direction**

In the YZ plane of our model, the large birefringence coefficient results in a greater separation of the fast and slow rays. Using the echo-dynamic plot in Figure 11 it is not possible to account for the peaks in amplitude with the probe at positions 2 and 4. There appears to be no peak response from the ray at the first V-path of the slow shear, yet a strong peak is seen at the position of the slow shear double-V position. Position 5 matches the ray path for the V-path of the fast shear.

It would be difficult for a person using the pitch-catch technique to identify the appropriate peak upon which to assess the refracted angle using the equation from DNV CN7.
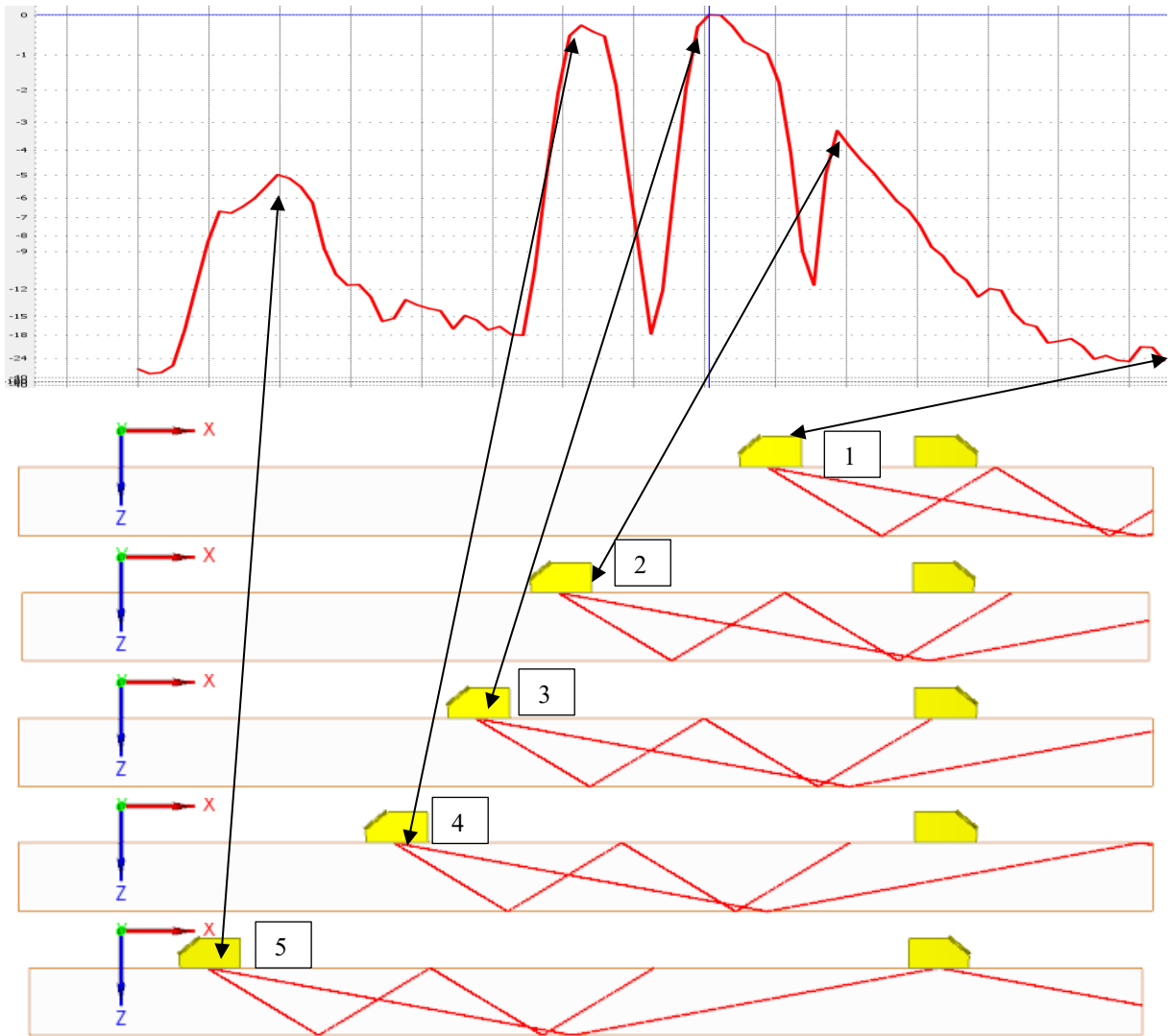
**Figure 11**      **Echo-dynamic of nominal 60° in anisotropic steel perpendicular to rolling direction**

To understand why the echo-dynamic plot does not follow the simple ray tracing, we need to consider the energy flow that results. The beam plot using the 10mm diameter probe on the nominal 60° refracting wedge does not indicate a double lobe beam with one centred at 59° and the other at 79.7°. Instead, Figure 12 shows that the main particle displacement follows a path indicated as 75° refracted.
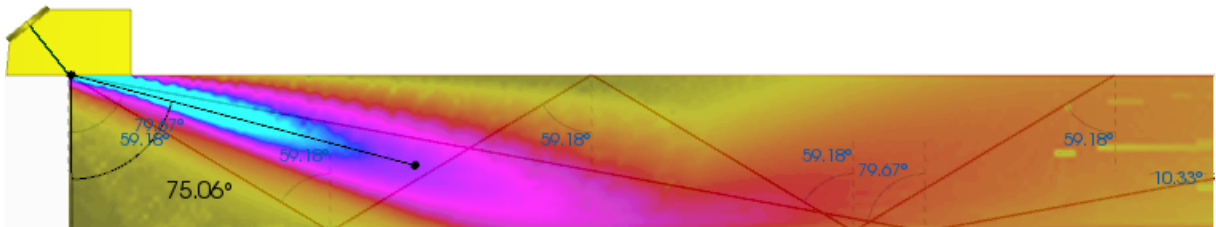


**Figure 12**      **Beam of a nominal 60° probe on anisotropic steel perpendicular to rolling**

If the degree of birefringence is not excessive, Holloway [10] demonstrated the pitch-catch approach could be carried out using phased-array probes. This allows the user to cover a range of angles, making it more beneficial to assess the useful angles that could be used.


# 6. Discussion

We have described how acoustically anisotropic materials can change velocities depending on the direction assessed. Generally, the effect is less pronounced on the longitudinal mode. For the transverse mode there is an added effect of birefringence; whereby a fast and slow shear mode forms with particle vibration at mutual right angles to each other. For weld inspection using angled beams, anisotropy will result in deviation of the beam from the assumed path that was determined on a basic isotropic reference block such as the ISO Calibration Block No. 1. The significance of deviation from the assumed path is that indications associated with flaws in the weld will be incorrectly plotted. Or even worse, it may be that the beam is refracted to the point that it is no longer in the test material; having been totally internally reflected in the wedge. Because refraction is more sensitive to acoustic velocity changes at higher incident angles, weld inspections using higher refracted angles are more likely to be affected.

For manual ultrasonic testing, incorrect positioning of a flaw is easily demonstrated. Having calibrated on a normal isotropic reference block with shear velocity 3240m/s, a nominal 60° probe would correctly place a lack of sidewall fusion on the lower bevel surface of a steel plate having acoustic velocity 3240m/s.
However, if the plate was actually anisotropic and the velocity 3410m/s, the refraction would be a bit greater and at the same standoff and sound path, the indication would be identified as a root defect or perhaps merely a bit of excess penetration as seen in Figure 13.
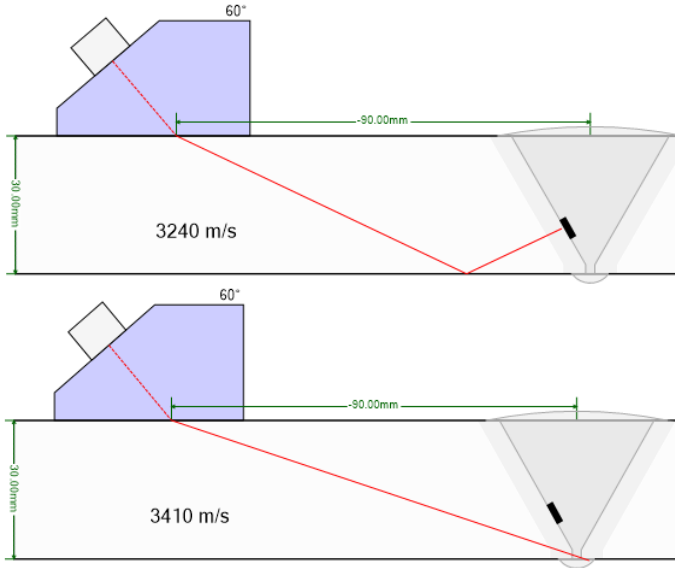


**Figure 13      Effect of velocity difference from reference calibration block**

When carrying out weld inspection on anisotropic materials, the beam is generally directed perpendicular to the weld axis. Determining the acoustic velocities in the plane of inspection will be critical to the detection and positioning of flaws. Using a 0° shear wave probe to obtain a fast and slow velocity through the thickness of the plate is not likely to provide adequate detail

of the range of velocities over the range of angles that will be used to inspect the weld. Pitch-catch configurations with monoelement or phased-array probes can provide better detail of the velocity variations with respect to angle. As well, the pitch-catch method can also provide the effect of energy flow, not available with the assessment using 0° shear wave probes on samples cut at various angles in the inspection plane.

A further complexity is introduced when welds are made at some oblique angle to the rolling direction. An example of this is when welds are used to join spiral seamed pipe. Then the beam is not aligned with either the rolling direction nor the direction at right angles to the rolling direction. In addition to altering the refracted angle, this can result in a skewing of the beam to the left or right of the direction that the probe is pointed.

## 7. Conclusions

CIVA helps to explain what is happening in inspections of anisotropic steel.
Having access to a horizontally polarised piezo-element in Civa, allows for the ability to confirm the acoustic properties predicted by the Christoffel equations.
CIVA can provide a means of assessing when the degree of anisotropy will become problematic to locate flaw indications in welds inspected with angled shear waves.
Velocity deviations due to anisotropy are seen to cause more pronounced effects on higher angles in shear mode.
When a high degree of anisotropy exists in the shear mode, small angles of refraction should be recommended or the use of compression mode may be a solution; however, it should be cautioned that using L-mode limits inspection to the first half-skip due to the regular concerns for mode conversion.

This paper assumed a constant acoustic anisotropy through the entire thickness of the steel plates simulated. This is probably a reasonable assumption for relatively thin plates; however, for thick sections the degree of texturing is likely to reduce towards the middle of the plate. It is recommended that future research be done to assess how this might affect inspections results.

## Acknowledgements

## References

1. ISO 2400:2012, Ultrasonic testing Specification for calibration block No. 1, ISO copyright office, Case postale 56 • CH-1211 Geneva 20
2. ISO 7963:2022, Non-destructive testing — Ultrasonic testing — Specification for calibration block No. 2, ISO copyright office, Case postale 56 • CH-1211 Geneva 20
3. ISO 19675:2017, Non-destructive testing — Ultrasonic testing — Specification for a calibration block for phased array testing (PAUT), ISO copyright office, Case postale 56 • CH-1211 Geneva 20

4. Keiji, I.B.A., Method of Ultrasonic Angle Beam Examination for Welds of Ferritic Steels with Acoustic Anisotropy, The Joint Research Society, Iron and Steel Institute of Japan, 1987
5. Ginzel, E., Holloway, P., Visualisation of Acoustic Birefringence, https://www.ndt.net/article/ndtnet/papers/Visualisation_of_Acoustic_Birefringence.pdf NDT.net, 2021
6. Linton Carvajal, Alfredo Artigas, Alberto Monsalve, Yolanda Vargas, Acoustic Birefringence and Poisson's Ratio Determined by Ultrasound: Tools to Follow-Up Deformation by Cold Rolling and Recrystallization, Mat. Res. 20 (Suppl 2) 2017  https://doi.org/10.1590/1980-5373-MR-2016-1082 , https://www.scielo.br/j/mr/a/yffpsDmZjn64YprwRqcJD8M/?lang=en#
7. P. Spalthoff, W. Wunnike, C. Nauer-Gerhard, H. J. Bunge, E. Schneider, Determination of the Elastic Tensor of a textured Low-Carbon Steel, Textures and Microstructures, 1993, Vol. 21, pp. 3-16, Gordon and Breach Science Publishers S.A.
8. E.A. Ginzel and R.K. Ginzel, "Study of Acoustic Velocity Variations in Line Pipe Steel", Materials Evaluation, May 1995, pp. 598-60
9. DNV ST-F101, "Submarine Pipeline Systems, Appendix E, Automated Ultrasonic Girth weld testing, 2021
10. P. Holloway, E. Ginzel, Calibration for Anisotropic Effects on Shear Wave Velocity for Improvements of Weld Inspections in TMCP Steels, https://www.ndt.net/article/ndtnet/papers/Calibration_for_Anisotropic_Effects_on_Shear_Wave_Velocity_for_Improvements_of_Weld_Inspections_in_TMCP_Steels.pdf
11. P. Holloway, https://www.youtube.com/watch?v=aPxKdGmMUmM
12. Classification Notes No.7, Non-destructive Testing, Det Norske Veritas, 2012